The Role of the Tunneling Matrix Element and Nuclear Reorganization in the Design of Quantum-dot Cellular Automata Molecules

Jackson Henry and Enrique P. Blair[1]
Baylor University

(Dated: 17 December 2017)

Mixed-valence molecules provide an implementation for a high-speed, energy-efficient paradigm for classical computing known as quantum-dot cellular automata (QCA). The primitive device in QCA is a cell, a structure with multiple quantum dots and a few mobile charges. A single mixed-valence molecule can function as a cell, with redox centers providing quantum dots. The charge configuration of a molecule encodes binary information, and device switching occurs via intramolecular electron transfer between dots. Arrays of molecular cells adsorbed onto a substrate form QCA logic. Individual cells in the array are coupled locally via the electrostatic electric field. This device networking enables general-purpose computing. Here, a quantum model of a two-dot molecule is built in which the two-state electronic system is coupled to the dominant nuclear vibrational mode via a reorganization energy. This model is used to explore the effects of the electronic inter-dot tunneling (coupling) matrix element and the reorganization energy on device switching. A semi-classical reduction of the model also is made to investigate the competition between field-driven device switching and the electron-vibrational self-trapping. A strong electron-vibrational coupling (high reorganization energy) gives rise to self-trapping, which inhibits the molecule's ability to switch. Nonetheless, there remains an expansive area in the tunneling-reorganization phase space where molecules can support adequate tunneling. Thus, the relationship between the tunneling matrix element and the reorganization energy affords significant leeway in the design of molecules viable for QCA applications.

I. INTRODUCTION

Mixed-valence multi-center molecules are being investigated for use in an energy-efficient, high-speed, general-purpose molecular computing paradigm known as quantum-dot cellular automata (QCA).[1–5] Here, a molecule serves as a primitive device known as a cell, from which more complex logic[3,4,6]—and indeed entire processors[7]—may be designed. Metal centers within a molecular cell provide redox centers, which function as quantum dots. Mobile charges may localize on dots within the molecule, and the configuration of mobile charges can be used to encode classical bits. The inter-dot quantum tunneling of charge enables device switching. QCA circuits, formed by adsorbing arrays of cells onto a substrate, are interconnected using the local electrostatic electric field. This field provides a bias to drive electron transfer within a molecule. Molecules such as diferrocenyl acetylene (DFA) and zwitterionic nido-carborane ($Fc^+FcC_2B_9{}^-$) are being investigated as candidates for this application.[8,9] DFA provides two quantum dots, forming the simplest type of QCA molecule. $Fc^+FcC_2B_9{}^-$ provides a three-dot molecule and enables the electric-field clocking of molecular QCA devices and circuits.

Molecular QCA devices have not yet been experimentally demonstrated, neither at the cellular level nor at the circuit level, and molecular properties that will optimize device operation remain unknown. While the processes of synthesis, imaging, and testing of concept QCA molecules are costly and time-consuming, insights may be gained quickly and inexpensively from predictive models of molecular QCA performance. Here, a model is developed to investigate two important features in a DFA-like molecular QCA candidate: its ability to support strong bits, and its ability to switch states. These are explored in terms of the electron transfer matrix element H_{AB} for charge tunneling between electronic states, and the reorganization energy λ coupling the molecule's electronic state to its own nuclear displacements. Low H_{AB} tends to localize the electronic state, leading to stronger bit values; and high H_{AB} enables electronic delocalization, leading to weaker bit values. Low λ decouples the electronic state from the vibrational state of the molecule, but high λ couples them and tends to localize the electron. Indeed, λ can become so strong that electron transfer is inhibited by the electron-vibrational self-trapping. This can preclude device switching, an important function in QCA logic. We show that there is a significant region in the (λ, H_{AB}) phase space over which self-trapping does not inhibit molecular device switching.

The investigation begins in Sect. II with a fully-quantum model for a QCA molecule's electronic state and the dominant molecular vibrational state. The quantum model also is reduced to a semi-classical model, which enables the exploration of the impact that self-trapping has on device switching. The fully-quantum model of Sect. III yields results consistent with those of a semi-classical model by Lu and Lent[11]. The semi-classical reduction of the fully-quantum model also demonstrates that the (λ, H_{AB}) phase space has a significant area over which the self-trapping does not inhibit switching in QCA molecules.

II. MODEL

A. Electronic Subsystem

A DFA-like QCA molecule has two quantum dots separated by distance a, and the charge configuration is modeled as a two-state electronic system. The localized electronic states (depicted in Fig. 1) provide a basis for the electronic system.

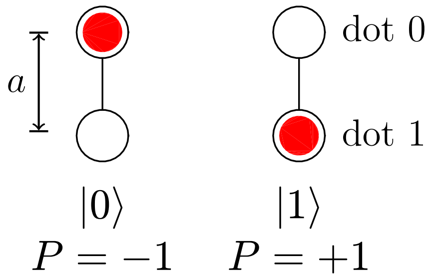

FIG. 1. Schematic representation of the localized electronic states $\{|0\rangle, |1\rangle\}$ of a two-dot QCA molecule. These states provide a basis for the electronic subsystem. Each black circle represents a quantum dot. The black line represents an electronic tunneling path between the interconnected dots. The red circle represents a mobile electron. The dots are separated by a distance a. A cell can have polarization $P = \pm 1$. Not pictured here is the molecule's fixed neutralizing charge.

The electronic system's Hamiltonian, $\hat{H}_e$, has the following form:

$$\hat{H}_e = -H_{AB}\hat{\sigma}_x + \frac{\Delta}{2}\hat{\sigma}_z. \tag{1}$$

Here, H_{AB} is the electronic coupling or the hopping energy between the $|0\rangle$ and $|1\rangle$ states, and Δ is the detuning between the $|1\rangle$ and $|0\rangle$ states:

$$\Delta = \langle 1| \hat{H}_e |1\rangle - \langle 0| \hat{H}_e |0\rangle . \tag{2}$$

Δ is determined by electrostatic interactions with neighboring cells. The operators $\hat{\sigma}_x$ and $\hat{\sigma}_z$ are two of the Pauli operators H_e:

$$\begin{aligned} \hat{\sigma}_x &= |0\rangle\langle 1| + |1\rangle\langle 0| , \\ \hat{\sigma}_y &= i\left(|0\rangle\langle 1| - |1\rangle\langle 0|\right), \text{and} \\ \hat{\sigma}_z &= -|0\rangle\langle 0| + |1\rangle\langle 1| \ . \end{aligned} \tag{3}$$

An energy useful in characterizing the system is the kink energy, E_k. E_k is the cost of a bit flip. This can be quantified as the magnitude of Δ when $P_{drv} = \pm 1$. Therefore, if $P_{drv} = \pm 1$, $E_k = 420$ meV.

We define a polarization, P, which quantifies the electronic configuration of a cell. P, the expectation value of $\hat{\sigma}_z$, may vary continuously over the interval $[-1, 1]$:

$$P = \langle \hat{\sigma}_z \rangle = \mathrm{Tr}(\hat{\sigma}_z \hat{\rho}_e). \tag{4}$$

Here, $\hat{\rho}_e$ is the density operator for the electronic subsystem.

B. Vibrational Subsystem

The vibrational subsystem is modeled using a quantum harmonic oscillator. The oscillator's position, Q, represents the reaction coordinate for the dominant vibrational mode of the molecule, assumed to be the antisymmetric breathing mode. The Hamiltonian for this system, $\hat{H}_v$, is given by

$$\hat{H}_v = \hbar\omega\left(\hat{a}_Q^\dagger \hat{a}_Q + \frac{1}{2}\right) = \frac{\hat{P}_Q^2}{2m} + \frac{1}{2}m\omega^2\hat{Q}^2, \tag{5}$$

where, $\hat{a}_Q$ and $\hat{a}_Q^\dagger$ are the annihilation and creation operators, respectively, for a vibron, a quantum of intramolecular vibration. Also, m denotes the oscillator's effective mass, and ω represents its angular frequency of oscillation. Eqn. (5) also expresses $\hat{H}_v$ in terms of the vibrational system's momentum operator $\hat{P}_Q$ and position operator $\hat{Q}$:

$$\hat{P}_Q = i\sqrt{\frac{m\omega\hbar}{2}}\left(\hat{a}_Q - \hat{a}_Q^\dagger\right) \ , \quad \text{and} \tag{6}$$

$$\hat{Q} = \sqrt{\frac{\hbar}{2m\omega}}\left(\hat{a}_Q + \hat{a}_Q^\dagger\right) \tag{7}$$

Here, the term $\hat{P}_Q^2/2m$ is the subsystem's kinetic energy operator, and $m\omega^2\hat{Q}^2/2$ is its potential energy operator.

C. A Fully-quantum Treatment of the Composite Electron-Vibration System

The Holstein molecular-crystal model[10] is used to treat the coupled electron+vibration system, with coupling term $\hat{H}_{ev}$, linear in both $\hat{\sigma}_z$ and $\hat{Q}$:

$$\hat{H}_{ev} = \frac{g_{ev}}{2}\hat{\sigma}_z\hat{Q}. \tag{8}$$

The electron-vibration coupling coefficient g_{ev} is related to the reorganization energy λ by

$$g_{ev} = \sqrt{2m\omega^2\lambda}. \tag{9}$$

This model is depicted schematically in Fig. 2. Here, neighboring molecules (represented as "external drivers" in the figure) establish an electrostatic electric field, which determines a potential—and thus the value of Δ—for the electronic system. The electronic system, then, is coupled via $\hat{H}_{ev}$ to the vibrational system.

The complete Hamiltonian for the electron+vibration system is the sum of the electronic Hamiltonian, the vibrational Hamiltonian, and the coupling:

$$H = -H_{AB}\hat{\sigma}_x + \frac{\Delta}{2}\hat{\sigma}_z + \frac{\hat{P}_Q^2}{2m} + \frac{1}{2}m\omega^2\hat{Q}^2 + \frac{g_{ev}}{2}\hat{\sigma}_z\hat{Q}. \tag{10}$$

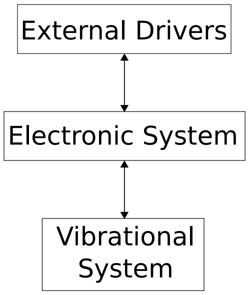

FIG. 2. An electric-field-driven QCA molecule is modeled using an electronic system coupled to the dominant vibrational mode of the molecule's nuclear coordinates. The "external drivers" component represents the influence neighboring molecules have on the target molecule's electronic state via the electrostatic electric field.

D. A Semi-classical Reduction of the Fully-quantum System

It will be useful to consider a semi-classical reduction of the Eqn. (10). In this limit, the vibrational kinetic energy is ignored, and the vibrational position operator $\hat{Q}$ is treated classically as a scalar value Q. Thus, the Hamiltonian of Eqn. (10) reduces to a semi-classical Hamiltonian $\hat{H}^{(sc)}$:

$$\hat{H}^{(sc)} = -H_{AB}\hat{\sigma}_x + \frac{\Delta}{2}\hat{\sigma}_z + \frac{1}{2}m\omega^2 Q^2 + \frac{g_{ev}}{2}\hat{\sigma}_z Q. \quad (11)$$

This model will the enable the exploration of the competition between field-driven device switching and the self-trapping of mobile charge on a particular quantum dot due to strong electron-vibron coupling.

III. RESULTS

Fig. 3 shows the cell-cell response curve, which is the response of a target cell to a driver cell. Here, the target cell polarization P is calculated from the cell's ground state given driver polarization P_{drv} and the Hamiltonian of Eqn. (10). The non-linear response is a signal gain, in which a weak P_{drv} results in a strong P. This effect is quantified using β, the steepness of the curve at center of the graph:

$$\beta \equiv -\left.\frac{dP}{dP_{drv}}\right|_{P_{drv}=0} . \quad (12)$$

The cell-cell response curve is shown for various values of the electronic coupling H_{AB}. Low values of H_{AB} lead to high electronic localization and a desirably high β with a strong polarization response in the target cell for a given P_{drv}. The numerical results shown here are consistent with previous analytic results by Lu and Lent.[11] While the work of Lu and Lent was based on the semi-classical model described by $\hat{H}^{(sc)}$, the results shown here are from the fully-quantum model described by $\hat{H}$ of Eqn. (10).

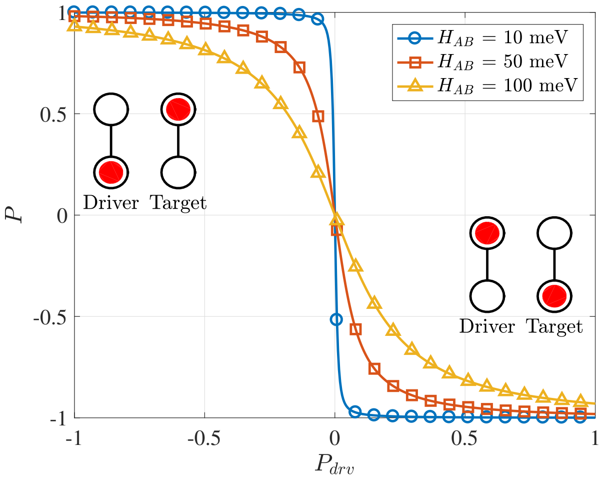

FIG. 3. The polarization response P of a target cell to a driver input P_{drv} is calculated by finding the ground state for Hamiltonian $\hat{H}$ for different values of electronic coupling H_{AB}. Increasing H_{AB} facilitates electron transfer and delocalization, but lower H_{AB} provides for better signal gain (higher β) and a stronger signal strength $|P|$. Here, parameters inspired by those of the DFA molecule were used: $a = 1$ nm, $m = 6$ amu, $f = 300$ cm^{-1}, and $\lambda = 100$ meV.

Increasing λ provides another means to increase signal gain and electronic localization, resulting in higher β and P values. This effect is shown in Fig. 4. When the electron is decoupled from the molecular vibrations ($\lambda = 0$), the resulting cell-cell polarization curve (blue line in Fig. 4) matches the cell-cell response when the vibrational subsystem is not considered (compare to the $H_{AB} = 50$ meV, shown in the yellow curve of Fig. (3). On the other hand, strong electron-vibration coupling ($\lambda = 400$ meV) gives to charge self-trapping on the dots, resulting in greater electronic localization and a stronger polarization magnitude $|P|$ for a given P_{drv}.

Fig. 5 highlights the competition between field-driven electronic switching and electron-vibrational self-trapping. The electric field due to the driver is varied by changing the electronic configuration of the driver molecule, but Q is fixed at a particular value $Q = Q_o$, with Q_o defined as

$$Q_o = \frac{g_{ev}}{2m\omega^2} . \quad (13)$$

Here, the semi-classical $\hat{H}^{(sc)}$ is used to calculate P as a function of P_{drv}, and this is repeated for various values of the reorganization energy λ. For low reorganization energy, the impact of this is minimal: the cell-cell polarization response demonstrates that both positive and negative output polarizations are possible over the full input domain $-1 \leq P_{drv} \leq +1$. For a larger value of λ, the

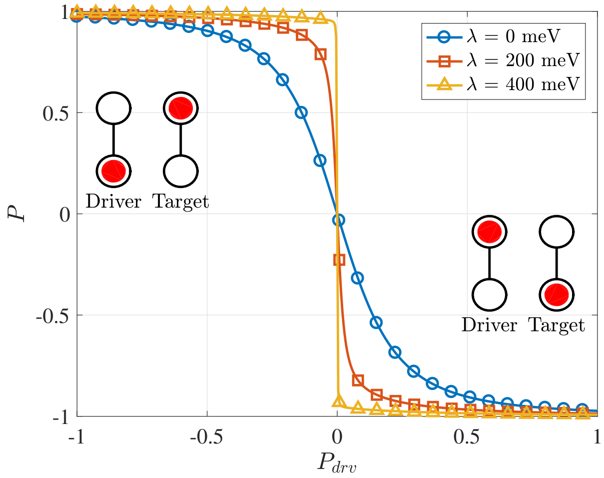

FIG. 4. Increasing λ enhances the cell's polarization response by creating a sharper transition in $P(P_{drv})$. Here, DFA-like calculation parameters were used: $a = 1$ nm, $m = 6$ amu, $f = 300$ cm^{-1}, and $H_{AB} = 50$ meV.

competing vibrational coordinate has a significant impact: the electron-vibration coupling is significant, self-trapping dominates, and the electric field from the driver molecule no longer is sufficient to switch the state of the target device. When $\lambda = 400$ meV, $P(P_{drv}) > 0$ for most of the domain. Even in the extreme upper input domain ($P_{drv} \to +1$), P attains only a slightly negative value. When $\lambda = 500$ meV, it is impossible over the valid input domain $P_{drv} \in [-1, 1]$ to drive a "0" bit ($P < 0$) on the target cell. The target cell is stuck in the "1" state ($P > 1$), a condition undesirable in molecular QCA devices.

Finally, the ability of the electronic system to switch is quantified by evaluating the change in output P over the two extreme values of the input P_{drv}, given vibrational coordinate $Q = Q_o$. We define the measure ΔP

$$\Delta P = \frac{1}{2}\left(P_{+} - P_{-}\right) \ , \tag{14}$$

where P_{+} is the target cell response for $P_{drv} = -1$, and P_{-} is the target cell response to $P_{drv} = +1$. Thus, $\Delta P = 0$ represents the extreme case of a cell unable to switch its electronic state, and a cell fully capable of switching has $\Delta P = 1$. Even $\Delta P \sim 0.5$ is undesirable in a cell, for such a cell with $P_{+} \sim 1$ will have $P_{-} \sim 0$. $\Delta P \geq\sim 0.8$ is more desirable, as a cell with $P_{+} \sim 1$ could be driven to $P_{-} \sim -0.6$.

A plot of ΔP as a function of λ and H_{AB} is given in Fig. 6. Since in QCA operation, it is desirable for $\Delta \gg H_{AB}$, we consider $0 \leq H_{AB} \leq 0.3 E_k$. The color gradient encodes the value of ΔP at each point (blue: $\Delta P \to 0$; yellow: $\Delta P \to 1$). This data demonstrates that there is a significant region within the phase space (λ, H_{AB}) in which the cell has an acceptable switching response. Here, field-driven electron transfer is largely unimpeded by self-trapping effects due to the vibrational coordinate $Q = Q_o$. A large continent of $\Delta P \geq\sim 0.8$ (yellow region) extends from the origin of the plot upward (for increasing H_{AB}) and rightward (for increasing λ).

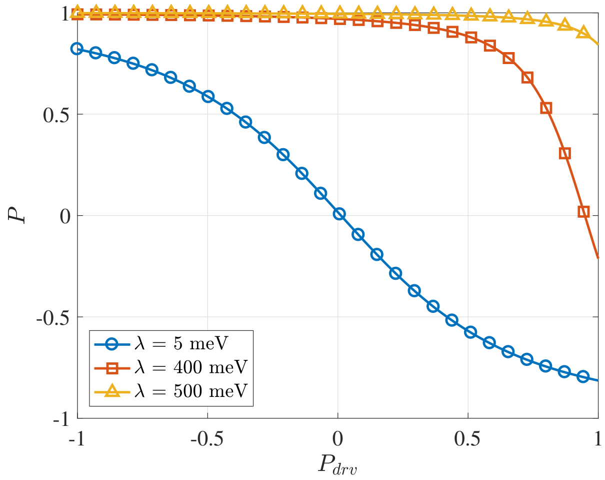

FIG. 5. High nuclear reorganization energy λ leads to self-trapping, which inhibits device switching. Polarization P is calculated for a cell with fixed vibrational coordinate $Q = Q_o$ in the semi-classical model for various values of λ. At low λ, the target cell's electronic state switches readily between $P < 0$ and $P > 0$ over the range of valid driver inputs, $P_{drv} \in [-1, 1]$. As λ increases, the nuclear coordinates are coupled more strongly to the electronic state, self-trapping becomes significant, and electronic switching in the molecule is degraded. Here, $H_{AB} = 0.15$ eV, $a = 1$ nm, $m = 6$ amu, and $f = 300$ cm^{-1}.

IV. CONCLUSION

Here, a fully-quantum model was developed for the electron+vibration configuration of a DFA-like, two-dot QCA molecule. The model reflects that decreasing H_{AB} or increasing λ provides for stronger device polarizations. A semi-classical reduction was made from the quantum model by ignoring nuclear kinetic energy and treating the reaction coordinate as a scalar value rather than a quantum mechanical operator. This reduction enables the modeling the effect of vibration-charge self-trapping on field-driven QCA device switching. Here, increasing λ more strongly couples the electronic state and the nuclear coordinates and may lead to the suppression of electronic tunneling (device switching) by self-trapping. Nonetheless, model showed that there is substantial freedom within the design phase space for QCA molecules to choose molecular parameters λ and H_{AB} and still expect adequate device switching.

Models such as the one presented here can play an important role in the realization of molecular QCA de-

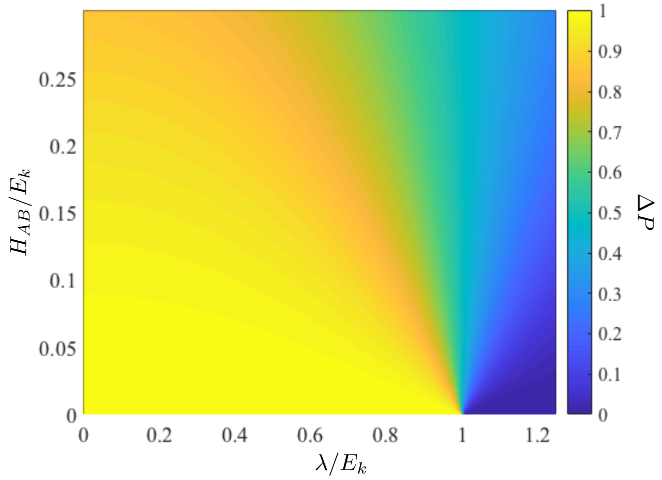

FIG. 6. ΔP quantifies the ability of a cell to switch states. Here, the reduced, semi-classical model is used, and a frozen nuclear coordinate $Q = Q_o$ is assumed. For low reorganization energy λ, the coupling between the electronic state and reaction coordinate is weak such that electronic switching between the ”0” state ($|1\rangle$ or $P = +1$) and the “1” state ($|0\rangle$ or $P = -1$) is largely unaffected: $\Delta P \simeq 1$. As λ grows, however, the fixed nuclear coordinates have a more significant effect on the molecule's electronic state, and switching is impeded ($\Delta P \to 0$). Nonetheless, there remains a large yellow region of the (λ, H_{AB}) phase space considered here in which a molecule switches well ($\Delta P \geq 0.8$). Here, $a = 1$ nm, $m = 6$ amu, and $f = 300$ cm^{-1}.

vices. Taking a concept molecule from design to synthesis, imaging, and testing is a high-latency, labor-intensive process of several personnel-years. On the other hand, models can highlight in a very quick and inexpensive manner those sets of molecular QCA properties which support effective device operation. This can accelerate the realization of molecular QCA devices by providing guidance in the design of QCA molecules, as well as allowing the community of researchers to avoid synthesizing unoptimized molecules.

This work is part of a larger effort to realize energy-efficient, high-speed molecular computation using molecular QCA. Some models already developed indicate the DFA-like molecules can support THz-speed device switching,[12] and that environmentally-driven quantum decoherence makes molecular QCA bits robust.[13,14] Other models are under development, especially models of power dissipation from QCA devices and circuits to the environment.

ACKNOWLEDGMENTS

This work was supported by an institutional start-up grant from Baylor University. The authors thank Craig Lent of the University of Notre Dame for insightful discussion.

[1] C. Lent, P. Tougaw, W. Porod, and G. Bernstein, “Quantum cellular automata,” Nanotechnology **4**, 49 (1993).
[2] C. S. LENT, P. D. TOUGAW, and W. POROD, “Bistable saturation in coupled quantum dots for quantum cellular automata,” Applied Physics Letters **62**, 714–716 (1993).
[3] P. Tougaw and C. Lent, “Logical devices implemented using quantum cellular automata,” J. Appl. Phys. **75**, 1818–1825 (1994).
[4] P. D. Tougaw and C. S. Lent, “Logical devices implemented using quantum cellular-automata,” J. Appl. Phys. **75**, 1818–1825 (1994).
[5] C. S. Lent, “Molecular electronics - bypassing the transistor paradigm,” Science **288**, 1597–+ (2000).
[6] M. Niemier and P. Kogge, “Logic in wire: Using quantum dots to implement a microprocessor,” in *NINTH GREAT LAKES SYMPOSIUM ON VLSI, PROCEEDINGS*, PROCEEDINGS - GREAT LAKES SYMPOSIUM ON VLSI, edited by R. Lomax and P. Mazumder (1999) pp. 118–121, 9th Great Lakes Symposium on VLSI (GLSVLSI 99), YPSILANTI, MI, MAR 04-06, 1999.
[7] M. Niemier and P. M. Kogge, “Problems in designing with qcas: Layout = timing,” Int. J. of Circ. Theor. App. **29**, 49–62 (2001).
[8] J. Christie, R. Forrest, S. Corcelli, N. Wasio, R. Quardokus, R. Brown, S. Kandel, Y. Lu, C. Lent, and K. Henderson, “Synthesis of a neutral mixed-valence diferrocenyl carborane for molecular quantum-dot cellular automata applications,” Angew. Chem. **127**, 15668–15671 (2015).
[9] R. C. Quardokus, N. A. Wasio, R. P. Forrest, C. S. Lent, S. A. Corcelli, J. A. Christie, K. W. Henderson, and S. A. Kandel, “Adsorption of diferrocenylacetylene on au(111) adsorption of diferrocenylacetylene on au(111) studied by scanning tunneling microscopy,” Phys. Chem. Chem. Phys. **15**, 6973–6981 (2013).
[10] T. Holstein, “Studies of polaron motion part i. the molecular-crystal model,” Ann. Phys.-New York **8**, 325–342 (1959).
[11] Y. Lu and C. Lent, “Field-induced electron localization: Molecular quantum-dot cellular automata and the relevance of robin–day classification,” Chem. Phys. Lett. **633**, 52–57 (2015).
[12] E. Blair, S. Corcelli, and C. Lent, “Electric-field-driven electron-transfer in mixed-valence molecules,” J Chem Phys **145**, 014307 (2016).
[13] E. P. Blair and C. S. Lent, “Environmental decoherence stabilizes quantum-dot cellular automata,” J. Appl. Phys. **113**, 124302 (2013).
[14] J. S. Ramsey and E. P. Blair, “Operator-sum models of quantum decoherence in molecular quantum-dot cellular automata,” J Appl Phys **122**, 084304 (2017).